Polymer 51 (2010) 3472–3485

Contents lists available at ScienceDirect

Polymer

journal homepage: www.elsevier.com/locate/polymer

Influence of polydopamine deposition conditions on pure water flux and foulant adhesion resistance of reverse osmosis, ultrafiltration, and microfiltration membranes

Bryan D. McCloskey [a], Ho Bum Park [b], Hao Ju [a], Brandon W. Rowe [a], Daniel J. Miller [a], Byeong Jae Chun [a], Katherine Kin [a], Benny D. Freeman [a,*]

[a] University of Texas at Austin, Department of Chemical Engineering, Center for Energy and Environmental Resources, 10100 Burnet Road, Building 133, Austin, TX 78758, USA
[b] Hanyang University, School of Chemical Engineering and WCU Department of Energy Engineering, Seoul 133-791, South Korea

ARTICLE INFO

Article history:
Received 10 November 2009
Received in revised form
28 April 2010
Accepted 1 May 2010
Available online 11 May 2010

Keywords:
Polydopamine
Membranes
Modification

ABSTRACT

The influence of polydopamine (PDOPA) deposition and poly(ethylene glycol) (PEG) grafting on pure water flux and bovine serum albumin (BSA) adhesion of two polysulfone ultrafiltration (UF) membranes, a poly(vinylidene fluoride) microfiltration (MF) membrane, and a polyamide reverse osmosis (RO) membrane is reported. When modified with PDOPA, all membranes exhibited a systematic reduction in protein adhesion. For example, 90 min of PDOPA deposition led to at least 96% reduction in BSA adhesion to these membranes at neutral pH. BSA adhesion was further reduced by subsequent PEG grafting to PDOPA (PDOPA-g-PEG). The membranes' pure water flux values (i.e., with no foulants present) were influenced to different extents by PDOPA and PDOPA-g-PEG modifications. In the porous membranes (i.e., the UF and MF membranes), the pure water flux reduction due to these modifications correlated with membrane pore size, with the smallest flux reductions observed in the MF membrane (e.g., <1% flux reduction for all PDOPA modification times considered), which have the largest pores, and the largest flux reductions occurring in UF membranes (e.g., a 40% flux reduction after 90 min of PDOPA deposition), which have pore sizes on the order of the PDOPA deposition thickness. The RO membranes, which are essentially non-porous, exhibited a flux reduction of 25% after 90 min of PDOPA deposition.

1. Introduction

Deposition of polydopamine (PDOPA), which is a newly discovered, bio-inspired polymer (i.e., so-called "bio-glue") [1], was found to reduce oil/water emulsion-induced fouling in a wide variety of water purification membranes, including poly(tetrafluoroethylene), poly(vinylidene fluoride), and polypropylene microfiltration (MF) membranes, polysulfone ultrafiltration (UF) membranes, and polyamide desalination membranes [2]. Moreover, amine-terminated poly(ethylene glycol) (PEG-NH_2) was readily grafted to PDOPA-modified membranes (called PDOPA-g-PEG modified membranes) which, in many cases, further improved fouling resistance [2].

Previously, PDOPA-g-PEG modified membranes were prepared using identical conditions for all membranes (1 mg/mL of 5 kDa PEG-NH_2 applied from aqueous solution at 60 °C for a period of 1 h for MF and UF membranes and 30 min for RO membranes) [2]. Such PEG grafting did not reduce pure water flux of PDOPA-modified MF membranes, and PDOPA-g-PEG modified MF membranes exhibited a higher flux during emulsified oil filtration than either PDOPA-modified or unmodified membranes [2]. For example, PDOPA and PDOPA-g-PEG modified PTFE MF membranes had 20% and 56% higher flux, respectively, than their unmodified analog after 1 h of emulsified oil/water filtration [2]. In contrast, PDOPA-g-PEG modification reduced pure water flux of UF and reverse osmosis (RO) membranes by more than 50% relative to that of their PDOPA-modified analogs. Consequently, PDOPA-g-PEG modified polysulfone ultrafiltration membranes (labeled PS-20 UF in Table 1) exhibited only slightly higher flux than PDOPA-modified PS-20 UF membranes during emulsified oil filtration. Similarly, although no flux decrease was observed during emulsified oil filtration, PDOPA-g-PEG modified RO membranes (labeled XLE RO in Table 1) exhibited fluxes lower than those of unmodified membranes that had been fouled. Based on these results, the current study was undertaken to explore the influence of PDOPA deposition and PEG grafting conditions on pure water flux in MF, UF, and RO membranes. The membranes considered in this study are listed in Table 1.

* Corresponding author. Tel.: +1 512 232 2803; fax: +1 512 232 2807.
E-mail address: freeman@che.utexas.edu (B.D. Freeman).

0032-3861/$ – see front matter © 2010 Elsevier Ltd. All rights reserved.
doi:10.1016/j.polymer.2010.05.008

Table 1
Membranes used in this study.

Classification	Polymer	Manufacturer (Membrane Name)	Pore Size	Study ID
RO	Interfacially polymerized aromatic polyamide	Dow Water & Process Solutions (XLE RO)	N/A	XLE RO
UF	Polysulfone	GE Infrastructure Water & Process Technologies (A1support)	~100 kDa MWCO	PSF A1 UF
UF	Polysulfone	Sepro Membranes, Inc. (PS-20)	~20 kDa MWCO	PS-20 UF
MF	Poly(vinylidene fluoride)	Millipore (GVHP)	0.22 μm	PVDF MF

Note: MWCO = molecular weight cutoff.

Protein adhesion has been explored in previous membrane fouling studies because of the presence of proteins in wastewater and bioprocessing streams and the aggressive nature of protein fouling of membranes [3–8]. In this study, PEG-NH_2 was grafted to a deposited PDOPA layer on the membrane surface to take advantage of the well-known protein adhesion resistance and fouling resistance properties of PEG [9]. To understand the ability of PDOPA and PDOPA-g-PEG surface treatments to modify the interaction of proteins with membranes, a static bovine serum albumin (BSA) adhesion test was used to characterize the influence of surface modification conditions on BSA adhesion. Further studies are under way to determine the protein fouling properties during dynamic filtration using PDOPA and PDOPA-g-PEG modified membranes, and results from these studies will be reported separately.

2. Theory

2.1. Hydraulic resistance of PDOPA and PDOPA-g-PEG modified membranes

In porous membranes, such as UF and MF membranes, water flux and transmembrane pressure (TMP) difference are related as follows [10]:

$$J_i = \frac{\Delta p}{\mu R_i} \tag{1}$$

where J_i is the steady-state water flux, Δp is the transmembrane pressure difference (TMP), μ is the feed solution viscosity, and R_i is the membrane's hydraulic resistance. In non-porous membranes (e.g., RO membranes), the solution–diffusion model is used to describe transport [11]:

$$J_i = A(\Delta p - \Delta\pi) \tag{2}$$

where A is the membrane's intrinsic water permeance, and $\Delta\pi$ is the osmotic pressure difference between the feed and permeate solutions. For non-porous membranes filtering pure water (i.e., $\Delta\pi = 0$), the hydraulic resistance is defined analogously to that shown in equation (1):

$$R_i = \frac{\Delta p}{\mu J_i} = \frac{1}{\mu A} \tag{3}$$

For both porous and non-porous membranes, the hydraulic resistance is determined experimentally as follows:

$$R_i = \frac{\Delta p \cdot t \cdot a}{\mu \cdot V} \tag{4}$$

where V is the volume of water collected during a time period t with a membrane of area a.

To quantify the effect of PDOPA modification and PEG grafting on membrane flux, an extension of equation (1) is employed for all membranes. PDOPA and PEG add resistances to the membrane's overall hydraulic resistance. A resistance in series model, having contributions from both the membrane and a PDOPA/PDOPA-g-PEG surface layer, can be expressed as [12]:

$$J_{PDOPA} = \frac{\Delta p}{\mu(R_o + R_{PDOPA})} \tag{5}$$

and

$$J_{PEG} = \frac{\Delta p}{\mu(R_o + R_{PDOPA} + R_{PEG})} \tag{6}$$

where J_{PDOPA} is the pure water flux of a PDOPA-modified membrane, J_{PEG} is the pure water flux of a PDOPA-g-PEG modified membrane, R_o is the unmodified membrane's hydraulic resistance, R_{PDOPA} is the hydraulic resistance of the PDOPA modification, and R_{PEG} is the hydraulic resistance of the PEG grafting layer. By combining equations (1), (5), and (6), R_{PDOPA} and R_{PEG} can be calculated as follows:

$$R_{PDOPA} = \frac{\Delta p}{\mu}\left(\frac{1}{J_{PDOPA}} - \frac{1}{J_o}\right) \tag{7}$$

and

$$R_{PEG} = \frac{\Delta p}{\mu}\left(\frac{1}{J_{PEG}} - \frac{1}{J_{PDOPA}}\right) \tag{8}$$

where J_o is the steady-state pure water flux through an unmodified membrane.

3. Materials and experimental methods

3.1. Materials

Dopamine hydrochloride, Trizma hydrochloride (i.e., tris buffer), isopropanol (IPA), sodium hydroxide, hydroxy-terminated poly(ethylene glycol) (PEG-OH, M_w = 3.35 kDa), sodium chloride, dimethyl sulfoxide, glycine buffer, and bovine serum albumin were purchased from Sigma Aldrich (St. Louis, MO, USA) and used as received. Flat-sheet XLE reverse osmosis (XLE RO) membranes were kindly provided by Dow Water & Process Solutions (Edina, MN, USA). Ultrafiltration polysulfone membranes (PSF A1 UF) with a nominal molecular weight cutoff of 92.5 kDa [12] were kindly provided by GE Infrastructure Water & Process Technologies (Minnetonka, MN, USA). Poly(vinylidene fluoride) microfiltration membranes (PVDF MF), with an average pore size of 0.22 μm, were purchased from Millipore (Cat. #GVHP, Billerica, MA, USA). Polysulfone ultrafiltration membranes were purchased from Sepro Membranes, Inc. (Cat. #PS-20 UF, Oceanside, CA, USA). Methyl-terminated poly(ethylene glycol) amine (PEG-NH_2, M_w = 5 kDa and 20 kDa) was purchased from JenKem, USA, Inc. (Allen, TX, USA) and Laysan Bio (Arab, AL, Mw = 1 kDa). Rhodamine N-hydroxyl succinimide (R-NHS), and slide-a-lyzers were purchased from Thermo Fisher Scientific Pierce Protein Research (Rockford, Il, USA). Sephadex columns were purchased from GE Life Sciences (Piscataway, NJ, USA). Ultrapure water (18.2 MΩ-cm) was obtained from a Millipore MilliQ Advantage A10 ultrapure water purification system.

3.2. Experimental methods

3.2.1. Water flux measurements on modified and unmodified membranes

Pure water flux was characterized in dead-end filtration cells (UHP43, Advantec MFS, Dublin, CA for MF and UF membranes; CF042, Sterlitech Corp., Kent, WA for RO membranes). Unmodified membranes were cut to the size appropriate for the dead-end cell to be used (UF and MF: 4.3 cm diameter, RO: 5.1 cm diameter) and immersed in IPA for at least 30 min prior to a flux measurement. The IPA soak insured that any extractable components (e.g., glycerin) were removed and that the porous structure of the UF and MF membranes was completely wetted. Relative to soaking the membranes initially in only water, this IPA pre-soak provided more reproducible water flux results, presumably because the IPA was more effective at insuring complete pore wetting in the hydrophobic UF and MF membranes considered in this study. Membranes were then placed in dead-end cells immediately after the IPA soak and rinsed with ultrapure water. Approximately 100 mL of ultrapure water was allowed to permeate through the MF and UF membranes and 30 mL through the RO membranes to rinse the IPA from the membrane structure before the water flux was measured. The pressure normalized pure water flux (in units of $L\ m^{-2}\ h^{-1}\ atm^{-1}$) for the unmodified UF and MF membranes was constant over a significant TMP range (i.e., 5–50 psi for UF, and 1–10 psi for MF). Extremely high throughput for the MF membranes limited testing at higher pressures. Similarly, the pressure limit ($\sim$50 psi) of the dead-end cells used in this study limited the TMPs tested for the UF membranes. All water flux experiments were performed at a fixed TMP (*e.g.,* MF membranes: 3 psi (0.2 atm), UF membranes: 10 psi (0.7 atm)) that was within the range of TMP values where pressure normalized flux was independent of TMP. On the other hand, the RO membrane TMP, which was 150 psi (10.2 atm), was selected based on a similar value used in a previous study [13].

After the unmodified membrane's pure water flux was measured, PDOPA modification was performed directly on the membrane coupon while it remained mounted in the dead-end permeation cell. 5–10 mL of aqueous dopamine solution (2 mg dopamine per mL of solution in 15 mM tris buffer at pH = 8.8 and ambient conditions) was added to each dead-end cell after decanting any remaining ultrapure water used for the flux measurement. Using magnetic stir bars, the dead-end cells were stirred intermittently during the PDOPA deposition process, and they were left open to air. After deposition, the membranes were carefully removed from the dead-end cells and rinsed with ultrapure water. They were then soaked in IPA, again for 30 min, to remove any unbound or loosely-bound PDOPA. The membranes were then placed in dead-end cells, and their pure water flux was measured as described previously. The membranes were then removed from the dead-end cells and modified by immersion in a PEG-NH_2 aqueous solution at the desired PEG-NH_2 concentration, temperature, and grafting time. Each PDOPA-g-PEG modification was performed in 15 mM Tris–HCl at pH = 8.8 buffer. Following PEG grafting, the membrane was removed from the solution and thoroughly rinsed under running ultrapure water. Afterwards, the water flux of the PDOPA-g-PEG membrane was recorded using the protocol described previously. This procedure allowed J_{PDOPA} and J_o to be measured for each individual membrane sample tested, which led to highly reproducible J_{PDOPA}/J_o values. This method was not used for protein adhesion experiments because a PDOPA modification could not be performed on an unmodified membrane that had been exposed to BSA. Therefore, another, more facile modification method, described below, was employed to prepare samples for the protein adhesion studies.

Stirred dead-end filtration is a poor technique to effectively analyze salt rejection of an RO membrane, because concentration polarization will lower rejection values under most conditions of operation of such filtration cells [13]. Therefore, salt rejection values in the RO membranes were not measured in this study. Dead-end filtration was used instead of crossflow filtration because it permits faster screening of samples, and the PDOPA modification could be performed easily inside the dead-end cell. However, previously, where salt rejection was measured in crossflow filtration, PDOPA deposition was found to have little effect on XLE RO salt rejection, and PDOPA-g-PEG modification actually increased membrane salt rejection [2].

3.2.2. PDOPA and PDOPA-g-PEG membrane modification for BSA adhesion measurements

Porous membranes (MF and UF) were prepared for PDOPA modification using the IPA immersion procedure outlined above, followed by immersion in ultrapure water for at least 30 min to exchange out the IPA from the membrane pores. RO membranes were soaked in ultrapure water at ambient conditions for at least 2 h prior to PDOPA modification.

A membrane was taped to a glass plate, and a glass ring (12 cm diameter) was secured to the membrane surface. 50 mL of the dopamine solution described in the previous section was placed in the glass ring (in contact with the membrane surface) and constantly stirred using a rocking platform shaker (Cat. #12620-906, VWR International LLC) at ambient conditions. The solution was exposed to air, as oxygen is required for the dopamine to PDOPA reaction to occur [1]. After the desired immersion period, the modified membrane was removed from the glass plate and thoroughly rinsed under running ultrapure water. Membranes were stored in ultrapure water until characterized for BSA adhesion or further modified to produce PDOPA-g-PEG modified membranes.

PEG conjugation (i.e., PDOPA-g-PEG modification) was accomplished as described above. Unless otherwise indicated, all PEG grafting was accomplished using a 2×10^{-4} mol/L PEG-NH_2 aqueous solution (i.e., 0.2 g/L of 1 kDa PEG, 1 g/L of 5 kDa PEG-NH_2, or 4 g/L of 20 kDa PEG-NH_2) at 60 °C. A Boekel Scientific incubator (Cat. # 133000, Feasterville, PA, USA) was used to keep the membrane and contiguous solution at constant temperature during the PEG grafting step. The standard grafting time was 60 min for MF and UF membranes and 30 min for RO membranes. Following grafting and rinsing, the membranes were stored in ultrapure water until characterized.

3.2.3. PDOPA deposition thickness measurements on polysulfone

To quantify the amount of PDOPA deposited on a surface as a function of immersion time, ellipsometry was employed on thin, non-porous films of bisphenol A-based polysulfone (PSF) from Solvay Advanced Polymers (UDEL PSF-3500 NT LCD) (Alpharetta, GA). Thin ($\sim$150 nm) films of polysulfone were prepared by spin coating a 3 wt% polysulfone solution in cyclopentanone onto silicon wafers at 1000 rpm [14]. Thickness was measured using a Model 2000D variable angle spectroscopic ellipsometer manufactured by J.A. Woollam Co.; the methods used to extract thickness information from these measurements have been described previously in refs. [15,16]. A polysulfone-coated wafer was then immersed in a stirred dopamine solution similar to that used to deposit PDOPA on membrane surfaces. After a desired deposition time, the polysulfone-coated wafer was removed from the dopamine solution, rinsed in running ultrapure water and air dried. The thickness of the coated polysulfone film was then measured using ellipsometry, and the PDOPA layer thickness was determined using a Cauchy model [16]. For the unmodified polysulfone films, a 3-layer model

was used to represent the system of a silicon substrate, a native silicon oxide layer, and the polysulfone film. A 4-layer model was used for the PDOPA-modified polysulfone films, where the 3 previously mentioned layers' properties were fixed based on the initial ellipsometry scan, and the 4th layer was used to model the PDOPA coating.

3.2.4. Contact angle measurements

Contact angle measurements were performed using a captive *n*-decane bubble in water, as described previously in Refs. [12]. A membrane was cut into a 5 mm wide strip and placed face down in a custom-made holder. The membrane-holder assembly was placed in a small, transparent water bath such that the membrane was fully immersed in water. A computer-controlled camera was focused on the membrane surface, and at least five *n*-decane bubbles were placed on the membrane surface using a syringe with a hooked needle. Images of the bubbles were analyzed using software from First Ten Angstroms (Portsmouth, VA, USA). The values reported in this study are the average and standard deviation of at least five measurements.

3.2.5. BSA adhesion measurements

Protein adhesion experiments were performed using a fluorimetric assay of tagged bovine serum albumin. R-NHS-tagged BSA, rather than fluorescein-tagged BSA, was used in this study because the desalination membranes exhibited a significant fluorescent signal at approximately the same excitation/emission spectrum as fluorescein. The fluorescent tagging of BSA was accomplished using a common approach [17]. Briefly, 40 mg of BSA was dissolved in 5 mL of ultrapure water, and 8 mg of R-NHS was dissolved in 175 μL of dimethyl sulfoxide. 150 μL of the R-NHS solution was added to the BSA solution and incubated at room temperature for 1 h, after which the reaction was quenched by adding 50 μL of glycine buffer. The reaction mixture was purified by elution through Sephadex columns and then dialysis against ultrapure water using Slide-A-Lyzers (15-20 h dialysis time was typical). The final concentration and fluorescent tags per BSA molecule were analyzed using UV spectrophotometry [17]. There were approximately 3.5 rhodamine molecules per BSA molecule.

2.5 cm (1 in.) diameter samples were cut from flat-sheet membranes. The circular samples were placed in dead-end cells (Advantec MFS, #UHP 25) having an effective surface area of 3.5 cm^2 and washed several times with ultrapure water. R-NHS-tagged BSA solution (0.1 mg/mL in ultrapure water, pH = 6.5) was then added to the cells. After 30 min, the protein solutions were decanted, and the membrane surface was washed repeatedly with ultrapure water. The membranes were then air dried, and their fluorescence intensity was measured (using either a fluorescent microscope (Leica DM IRBE, Bannockburn, IL, USA) or a plate reader (Tecan Sapphire II, Mannedorf, Switzerland)).

3.2.6. Gravimetric analysis to quantify PEG grafting density

Gravimetric analysis was performed using a Magnetic Suspension Balance (MSB, Rubotherm, Bochum, Germany). The amount of mass deposited on the membranes during PDOPA deposition was too low to be accurately detected by this gravimetric technique. Ellipsometry was found to be a more accurate technique for determining the amount of PDOPA deposited on thin PSF films. However, the amount of PEG deposited on the membrane was easily detectable using gravimetric analysis. Therefore, gravimetric analysis enabled the determination of grafting densities on actual membranes, rather than being limited (as in the ellipsometry studies) to characterization of flat, non-porous PSF films. PDOPA-modified membranes were cut into 1-inch diameter disks and soaked in IPA for at least 1 h. The membranes were then transferred to water for 1 h and dried under vacuum for at least 1 h at 50 °C. Typically, 6 membrane disks were stacked into the MSB sample holder and weighed at ambient conditions. Afterwards, PEG was grafted to the membrane by placing the membranes in a petri dish with a PEG-NH_2 solution. Following PEG grafting, the membranes were rinsed using water and IPA; in this step, they were immersed in IPA for at least 1 h. The membranes were then vacuum dried and reweighed. The difference in membrane weight before and after PEG grafting was ascribed to PEG grafted to the membrane surface. The PEG grafting density was calculated as the mass difference between PDOPA-modified and PDOPA-g-PEG modified membranes divided by the membrane nominal surface area determined by the diameter (1 in.) of each membrane coupon (i.e., area per coupon = 0.78 in^2) [2].

3.2.7. Ultrafiltration membrane pore size determination

To calculate the effective pore sizes of the UF membranes considered in this study, the membranes were challenged with dilute aqueous solutions (1 wt.%) of PEGs with various molecular weights (1–200 kDa). The membrane's mean pore diameter was taken to be equal to the Stokes diameter of the PEG exhibiting 50% rejection, which could be calculated from the molecular weight of the PEG using equation (9) [18]:

$$d = 33.46 \times 10^{-3} M_w^{0.557} \quad (9)$$

where d (nm) is the Stokes diameter of PEG of molecular weight M_w. The PEG concentrations in the feed and permeate solutions were measured using a total organic carbon (TOC) analyzer (Model TOC5050A, Shimadzu, Japan).

4. Results and discussion

4.1. Polydopamine modification of XLE RO, PS-20 and PSF A1 UF, and PVDF MF membranes: pure water flux

Fig. 1 presents pure water permeance (i.e., pressure normalized flux) of a PSF A1 UF membrane as a function of exposure time to a PDOPA solution (i.e., PDOPA deposition time). These data were collected using a procedure reported in ref. [2]. At short deposition times, permeance decreases strongly as PDOPA deposition

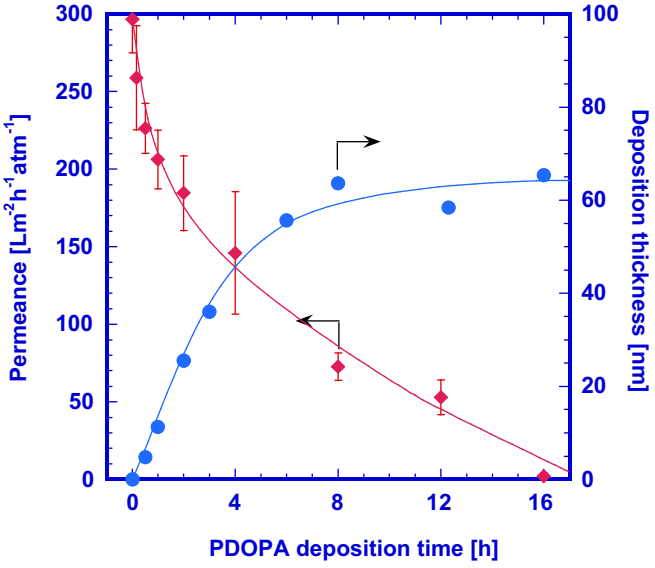

Fig. 1. Pure water permeance as a function of PDOPA deposition time on a polysulfone ultrafiltration membrane (PSF A1 UF), and PDOPA deposition thickness as a function of PDOPA deposition time on Udel polysulfone thin films [2].

time increases. For example, permeance decreased from 297 Lm^{-2} h^{-1} bar^{-1} to 2.2 Lm^{-2} h^{-1} bar^{-1} after 16 h of deposition. Fig. 1 also presents the influence of deposition time on PDOPA deposition thickness, as measured using ellipsometry [15,16], on thin, non-porous Udel PSF films. PDOPA deposition increased with increasing time, but appeared to approach a plateau of approximately 65 nm after about 8 h. Similar results (i.e., significant deposition at short exposure times to dopamine, followed by little deposition at long exposure times) were observed on silicon substrates [1,19]. 65 nm of PDOPA deposition corresponds to a very small fraction of the dopamine initially present in the solution (<1%), so the plateau in deposition thickness (cf., Fig. 1) is not a result of all of the dopamine depositing on the polysulfone film surface. Furthermore, the PDOPA solution remained dark brown, with visible formation of PDOPA particles after approximately 1 h, indicating reaction of dopamine in the solution. The plateau in deposition thickness presumably reflects the competition between PDOPA deposition and PDOPA formation in solution to consume free dopamine. In support of this hypothesis, Lee et al. observed that immersing a substrate in a PDOPA solution that had been previously incubated for long periods of time (greater than three days) led to no surface deposition [1].

The deposition thicknesses were in the same range as the pore size of the unmodified PSF A1 UF membrane, which was characterized using PEG molecular weight cutoff (MWCO) experiments (cf., Fig. 2). Typically, the mean pore diameter of a membrane is assessed as the Stokes diameter of the PEG molecule having a rejection of 50% [18]. For the PSF A1 UF membrane, the rejection is 50% for a 17.5 kDa PEG molecule, which, using equation (9), yields a pore diameter of 7.7 nm. To provide some characterization of the pore size distribution, the PSF A1 UF molecular weight cutoff (i.e., the PEG molecular weight for which the rejection was 90%) was 92.5 kDa [12], corresponding to a pore diameter of 18 nm [18].

During initial stages of deposition, PDOPA should be able to penetrate into the porous structure of the UF membrane because its molecular weight is still relatively low. Therefore, some PDOPA deposition probably occurs within the membrane pore structure, leading to pore constriction and an exponential decrease in water

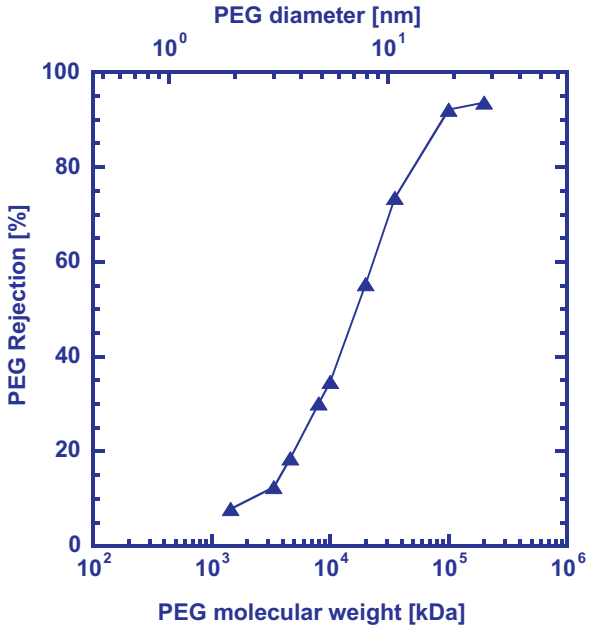

Fig. 2. Effect of PEG molecular weight on rejection by an unmodified PSF A1 UF membrane. From these data, the molecular weight cutoff is approximately 92.5 kDa. Adapted from Ref. [12].

Table 2
Influence of PDOPA deposition time on captive *n*-decane-in-water contact angles of PSF A1 UF membranes.

PDOPA deposition time [min]	Contact angle [°]
0	109 ± 5
10	49 ± 7
60	49 ± 4
120	58 ± 2
240	47 ± 5
480	47 ± 1
720	53 ± 4
960	55 ± 7

permeance, which is expected according to the Kozeny–Carman equation. However, as deposition time increases, the effective PDOPA molecular weight has been reported to reach millions [1]. Eventually, the thickness of the PDOPA layer may block the pores in the UF membrane, leading to the continuing decrease in membrane permeance observed in Fig. 1 at long deposition times. Although the PDOPA deposition thickness appears to plateau around a deposition time of 8 h, the flux of the UF membrane continues to decrease at longer deposition times (e.g., from 73 Lm^{-2} h^{-1} bar^{-1} at a deposition time of 8 h–2.2 Lm^{-2} h^{-1} bar^{-1} at a deposition time of 16 h). At 8 h, many pores have probably been significantly constricted, as observed by the significant reduction in permeance compared to that of unmodified membranes. Therefore, even small amounts of further PDOPA deposition, as is likely to occur at deposition times greater than 8 h, may bridge and completely block the pores, leading to substantial further decreases in membrane permeance. For water filtration applications, high water flux is desirable, so short PDOPA deposition times were the focus of this study, because they led to higher values of pure water flux.

Interestingly, even at low PDOPA deposition times, when the water flux of a PDOPA-modified membrane is only slightly less than that of an unmodified membrane, a significant increase in membrane surface hydrophilicity was observed. Table 2 presents captive *n*-decane bubble-in-water contact angles as a function of PDOPA deposition time for a PSF A1 UF membrane. At even the shortest deposition time considered, 10 min, the contact angle decreased significantly, indicating an increase in membrane hydrophilicity. All PDOPA-modified membranes exhibited similar contact angles after only brief deposition times. Membrane fouling resistance has been correlated with membrane surface hydrophilicity [20], so more hydrophilic surfaces should be more resistant to, for example, fouling by emulsified oil droplets.

Some further examples of the influence of PDOPA treatment on contact angles are presented in Table 3 for XLE RO membranes and PVDF MF membranes. These membranes are hydrophilic even before PDOPA modification. Even so, the XLE RO membranes showed a slight increase in hydrophilicity (i.e., a decrease in contact angle) following PDOPA modification. The PVDF MF membranes were even more hydrophilic than the XLE RO membranes initially. Because PVDF is not expected to be hydrophilic based upon its chemical structure, these membranes presumably contained hydrophilic surface-active additives (one such common additive is

Table 3
Captive *n*-decane-in-water (XLE RO) and air-in-water (PVDF MF) bubble contact angles.

	Contact Angle [°]	
Sample	Unmodified	PDOPA-modified
XLE RO	45 ± 3	36 ± 4
PVDF MF	31 ± 1	31 ± 4

Note: For the PVDF MF membranes, air-in-water bubbles were used because *n*-decane would readily sorb into the porous membrane structure of the unmodified membranes. The PDOPA deposition time was 60 min.

poly(vinyl pyrrolidone)[21]) in the PVDF membrane casting mixture to render the membrane surface hydrophilic. Because PVDF membranes had highly hydrophilic surfaces prior to PDOPA treatment, there was no discernable increase in their hydrophilicity due to PDOPA treatment.

To provide an indication of the relative decrease in pure water flux resulting from PDOPA deposition, Fig. 3 presents the influence of PDOPA deposition time on the fractional flux loss due to dopamine treatment, which is reported as the ratio of pure water flux of a PDOPA-modified membrane, J_{PDOPA}, to that of an unmodified analog, J_o. Each membrane responds differently to PDOPA modification. For example, PVDF MF membranes exhibited virtually no flux loss due to PDOPA modification. XLE RO membranes showed some flux loss, and the PS-20 UF membranes exhibited the largest decrease in flux with respect to deposition time. The PS-20 UF response is similar to the decrease observed for the PSF A1 UF membranes.

The differences shown in Fig. 3 may be rationalized by considering each membrane's structure. The PVDF MF membranes have a nominal pore size of 0.22 μm, which is more than an order of magnitude larger than that of the PSF A1 UF membranes discussed earlier. Based on the deposition thickness results for polysulfone, the PDOPA thickness, even after 90 min of deposition, should be much smaller than the nominal pore size of the PVDF MF membranes. Therefore, any pore size decrease associated with PDOPA modification should be negligible, so the pure water flux was not measurably influenced by modification.

During PDOPA deposition on PVDF MF membranes, PDOPA pore penetration was believed to be more pronounced than in the PSF A1 or PS-20 UF membranes, because the PDOPA polymerization solution was observed to permeate through the MF membrane during the deposition process. Therefore, deposition likely occurred throughout the porous structure of the PVDF MF membrane. Consistent with this hypothesis, the pure water flux of other, more hydrophobic MF membranes (e.g., poly(tetrafluoroethylene) (PTFE) and polypropylene (PP)) actually increased following PDOPA modification [2]. For example, J_{PDOPA}/J_o values for PTFE and PP MF membranes were 1.30 and 1.10, respectively, after 60 min of PDOPA deposition. Because PDOPA modification occurs under aqueous conditions and is believed to occur via a mild oxidation mechanism similar to that involved in melanin formation [1], PDOPA polymerization should not chemically degrade the membrane. Therefore, this flux increase should not be a result of membrane pore structure destruction. We speculate that an increase in membrane wettability, due to PDOPA deposition on the pore walls, coupled with a negligible decrease in the membrane's effective pore diameter, led to an increase in pure water flux. Presumably, the PDOPA treatment permitted wetting of some pores in the highly hydrophobic PTFE and PP membranes that might not otherwise have been wetted without PDOPA treatment, thereby opening additional transport pathways in the membranes. This wetting effect was less pronounced in the already hydrophilic PVDF MF membranes where, as indicated in Fig. 3, the J_{PDOPA}/J_o ratio is quite close to 1.

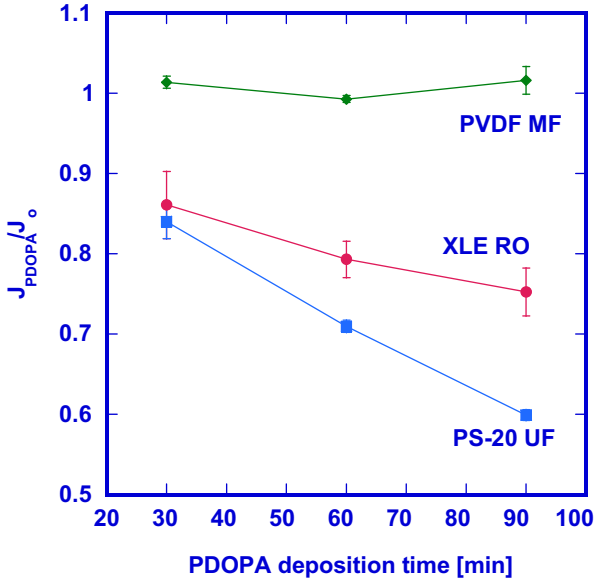

Fig. 3. The influence of PDOPA deposition time on the ratio of PDOPA-modified membrane pure water flux (J_{PDOPA}) to unmodified membrane pure water flux (J_o). Error bars represent standard deviations from at least 3 separate experiments.

Visually, PDOPA treatment changes the color of membranes. For example, PVDF MF and PS-20 UF membranes turn brown during PDOPA deposition. The XLE RO membranes had the least PDOPA deposition, since only a slight change in membrane color accompanied PDOPA deposition. PDOPA deposition occurred only on the surface of RO membrances as a result of the membranes' nonporous nature, so any flux reduction (or mass transfer resistance increase) associated with the deposition resulted from water transport through a thin PDOPA surface layer and not via pore constriction/blockage, as was the case in the porous UF and MF membranes. However, the polyamide RO layer was still believed to be the rate-controlling step in water transport through the modified membrane. Therefore, an increase in PDOPA deposition, due to increasing deposition time, resulted in only a small reduction in pure water flux. For example, as shown in Table 4, the PDOPA hydraulic resistance (R_{PDOPA}, equation (7)) on an XLE membrane ranged from 700×10^{10} m^{-1} (30 min deposition time) to 1000×10^{10} m^{-1} (90 min deposition time), which was significantly lower than the unmodified RO membrane's resistance, which was 3400×10^{10} m^{-1}.

4.2. PEG grafting to PDOPA-modified XLE RO, PS-20 UF, and PVDF MF membranes

4.2.1. Influence of grafting conditions on grafting density and pure water flux

Prior to PEG grafting, the PDOPA-modified membranes were prepared using a PDOPA deposition time of 60 min and the deposition conditions set forth in the Materials and Experimental Methods section. Fig. 4a presents the influence of PEG grafting temperature on the ratio of pure water flux of PDOPA-g-PEG modified PS-20 UF membranes, J_{PEG}, to that of their PDOPA-modified analogs, J_{PDOPA}. 5 kDa PEG-NH_2 was used for these studies. Temperature was varied in these PEG grafting to PDOPA-modified membranes because it is an important parameter that can be used to vary extent and rate of modification in both laboratory scale and large-scale membrane modifications. The temperature range in Fig. 4a was selected because it could be used on both laboratory and

Table 4
Influence of PDOPA deposition on membrane hydraulic resistance.

Membrane	Hydraulic Resistance $\times 10^{-10}$ (m^{-1})		
	PVDF MF	PS-20 UF	XLE RO
Unmodified, R_o	3.9	17.3	3400
PDOPA modified, R_{PDOPA}			
30 min	3.8	20.5	4100
60 min	4.0	24.8	4250
90 min	3.8	29.3	4400

Note: All values were calculated using equation (3).

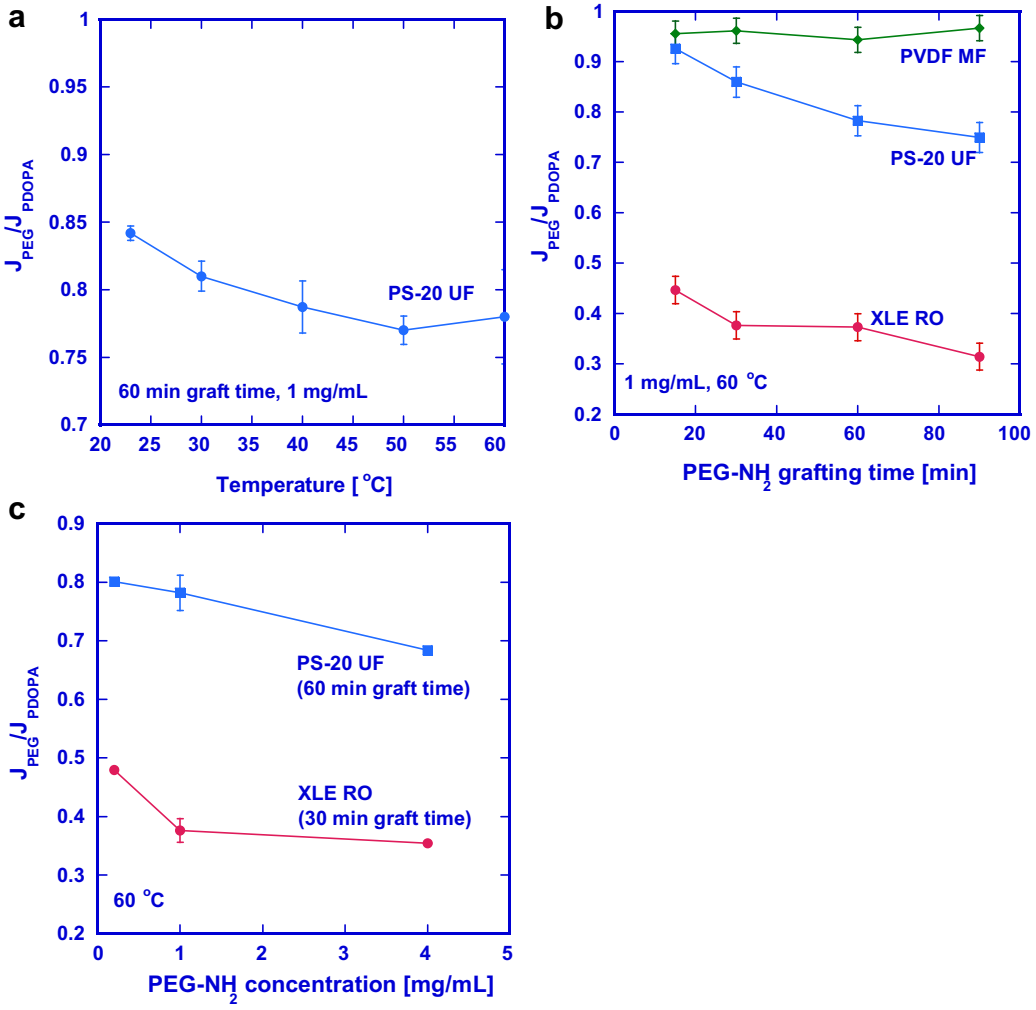

Fig. 4. The ratio of pure water flux of PDOPA-g-PEG modified membranes, J_{PEG}, to the pure water flux of PDOPA-modified membranes, J_{PDOPA}, as a function of: a) PEG grafting temperature, b) PEG grafting time, and c) PEG-NH_2 concentration in the grafting solution. A 60 min PDOPA deposition (2 mg/mL dopamine, 15 mM tris, pH = 8.8, ambient conditions) was used for all membranes prior to PEG grafting. All PEG grafting was performed using 5 kDa PEG-NH_2 in 15 mM tris buffer at pH = 8.8.

large-scale membrane modifications without damaging the membranes. The pure water flux was lower in all cases following PEG grafting (i.e., $J_{PEG}/J_{PDOPA} < 1$). This reduction in flux presumably occurred because the pore size of the UF membrane is on the order of the size of the PEG molecules used for grafting (e.g., the PS-20 rejection of 20 kDa PEG is 95%[22]). Therefore grafting most likely led to a combination of pore constriction and pore blockage (due to grafting on the membrane surface), which, in turn, increased the resistance to water transport. However, the extent of flux reduction due to PEG grafting was only weakly dependent on temperature because the flux reduction in PS-20 following PEG grafting changed by less than 10% (i.e., from $J_{PEG}/J_{PDOPA} = 0.84$ to 0.77) as temperature changed from 20 to 60 °C. This result suggests that the extent of PEG grafting did not change appreciably with temperature. The effect of temperature on PEG grafting was not explored for the other membranes considered in this study.

PDOPA deposition was necessary to achieve significant grafting of PEG-NH_2 to PS-20 UF membranes. For example, a PS-20 UF membrane not subjected to PDOPA deposition prior to being exposed to a 1 mg/mL 5 kDa PEG-NH_2 solution (pH = 8.8) for 60 min at 60 °C exhibited a flux decline of only 5% relative to that of an unmodified membrane (i.e., $J_{PEG}/J_o = 0.95$), indicating minimal PEG-NH_2 grafting to an unmodified PS-20 UF membrane. In contrast, the observed flux loss due to PEG grafting, under similar conditions, to a PDOPA-modified membrane was 22% (i.e., $J_{PEG}/J_{PDOPA} = 0.78$). Thus, PEG-NH_2 does not readily react with or strongly adsorb to unmodified PS-20 UF membranes. Similarly, grafting or adsorption of PEG-NH_2 to unmodified PVDF MF membranes was not expected to occur and was not explored in this study. PEG-NH_2 grafting to unmodified XLE RO membranes is discussed in detail below.

In the case of the PS-20 UF membranes, physical adsorption of PEG to PDOPA-modified membranes was not sufficient to cause a measurable flux decrease. For example, a PDOPA-modified PS-20 UF membrane was exposed to an aqueous solution containing 1 mg/mL of 3.35 kDa PEG-OH for 1 h at a pH of 8.8 and 60 °C. Unlike PEG-NH_2, PEG-OH cannot form covalent bonds with PDOPA. Such a membrane exhibited no flux decline ($J_{PEG}/J_o = 1.0$), indicating that physical adsorption of PEG to PDOPA is negligible. Therefore, the flux loss observed in Fig. 4 was ascribed to PEG that was covalently bound to PDOPA. This effect was not explored for PDOPA-modified PVDF MF and XLE RO membranes.

Fig. 4b presents the influence of PEG grafting time on the ratio of the pure water flux of several PDOPA-g-PEG modified membranes to that of their PDOPA-modified analogs. All results presented in this figure resulted from 60 min of exposure to PDOPA solution. PEG grafting did not significantly influence the PVDF MF membrane flux, as evidenced by only a ~3% flux decrease observed at any

grafting time considered. The PS-20 UF membranes exhibited a decrease in flux with increasing PEG grafting time, suggesting that PEG grafting density increased with increasing grafting time. This hypothesis was confirmed by gravimetric analysis described in greater detail below.

The XLE RO membranes exhibited the most significant flux reduction due to PEG grafting. For example, an XLE RO membrane was modified by exposure for 60 min to dopamine solution and then exposed to the PEG solution for 15 min to graft PEG to the PDOPA-modified surface. This modification led to a considerable decrease in flux ($J_{PEG}/J_{PDOPA} = 0.45$). However, at grafting times ranging from 15 to 90 min, the flux decrease was only weakly influenced by grafting time, since the flux decrease, J_{PEG}/J_{PDOPA}, only varied from 0.45 to 0.32. Presumably, most of the PEG grafting occurred at low grafting times (i.e., less than 15 min). PEG grafting to polyamide membranes is known to cause a decrease in membrane flux similar to or even greater than that observed in this study. For example, Mickols [23] observed a flux decrease of 80% (i.e., $J_{PEG}/J_o = 0.20$) for an FT-30 Dow Filmtec RO membrane modified using an aqueous solution containing 1 wt% PEG diepoxide (3.4 kDa), and he observed a flux decrease of 68% (i.e., $J_{PEG}/J_o = 0.32$) when an FT-30 membrane was modified by exposure to 0.2 wt% PEG diepoxide (0.2 kDa) solution. In both cases, the grafting time was 10 min, and the grafting temperature was 60 °C.

The influence of PEG-NH_2 solution concentration on pure water flux for 60 min PDOPA-modified PS-20 UF and XLE RO membranes is presented in Fig. 4c. Results for PVDF MF membranes are not presented because, based on the results presented in Fig. 4b, there was no systematic decrease in flux following PEG-NH_2 grafting, so these studies were not conducted for the PVDF MF membranes. A modest decrease in flux was observed at increasing PEG-NH_2 concentration for both PDOPA-modified PS-20 UF and XLE RO membranes, suggesting an increase in PEG grafting density with increasing PEG-NH_2 concentration. For the PS-20 UF membrane, whose grafting density was measured directly using a gravimetric technique, the increase in PEG grafting density with increasing PEG-NH_2 concentration was consistent with the gravimetric measurements, as will be described below.

Fig. 5 presents gravimetric measurements of grafting density of 5 kDa PEG-NH_2 on a PDOPA-modified PS-20 UF membrane. In this figure, the effect of PEG grafting time and PEG-NH_2 grafting solution concentration on grafting density is reported. The grafting density is reported as the mass of PEG added to the membrane per unit nominal surface area. In Fig. 5a, the PEG-NH_2 solution concentration was 1 mg/mL, and the grafting experiments were conducted at 60 °C and a solution pH of 8.8. In Fig. 5b, the influence of PEG-NH_2 solution concentration on grafting density was studied in membranes subjected to 60 min of PEG grafting at 60 °C and a pH of 8.8. These experiments were conducted at conditions to match those of the PS-20 UF flux measurements reported in Fig. 4b and c. PDOPA deposition was necessary to obtain appreciable grafting densities, because unmodified PSF UF membranes exposed to 5K PEG-NH_2 for 60 min exhibited very low PEG grafting densities (<1 μg cm^{-2}). Increasing grafting time and PEG-NH_2 solution concentration increases PEG grafting density. The effect of PEG grafting time and PEG-NH_2 grafting solution concentration on grafting density was not explored for PVDF MF or XLE RO membranes, although similar trends to those observed for PS-20 UF membranes would be anticipated. The observed increase in grafting density decreases the PS-20 UF membrane flux (as observed in Fig. 4b and c), possibly due to pore constriction and pore blockage associated with the increase in grafting. As will be shown later, all PEG grafting densities led to similar reductions in BSA adhesion.

Due to the rough surface and porous nature of membranes, apparent PEG grafting densities observed on membranes are significantly higher than grafting densities reported on smooth, non-porous surfaces. For example, on a smooth, non-porous surface, grafting densities as low as 0.033 chains per nm^2 for 5 kDa PEG (which corresponds to 0.027 μg/cm^2) are sufficient to cause overlap between the areas occupied by adjacent PEG chains (assuming a radius of gyration of 3.1 nm for a 5 kDa PEG molecule) [24]. At this grafting density, protein adhesion is greatly reduced due to steric repulsion. In our studies, much higher apparent grafting densities (for example, 30 μg/cm^2 for 5 kDa PEG-NH_2, 4 mg/mL, 60 °C, pH = 8.8 on a 60 min PDOPA-modified membrane) were observed on PS-20 UF membranes. However, this large graft density probably results from the membrane's surface roughness and internal porous structure, which substantially increases the total surface area above that of the nominal surface area, which is based on the surface area of the membrane if it were non-porous

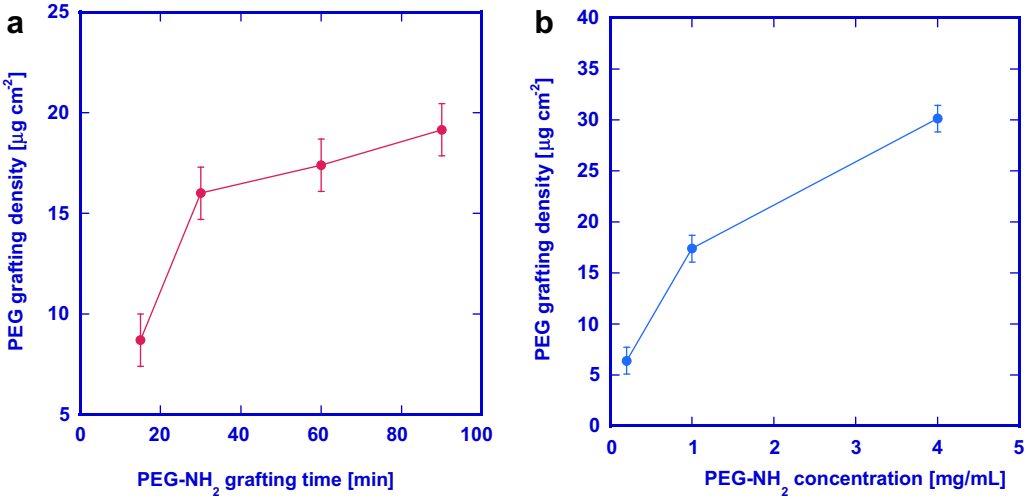

Fig. 5. PEG grafting density on PDOPA-modified PS-20 UF membranes as a function of: a) PEG-NH_2 grafting time, and b) PEG-NH_2 concentration in the grafting solution. Grafting conditions for a) 1 mg/mL 5 kDa PEG-NH_2, 60 °C, 15 mM tris buffer (pH = 8.8), and b) 60 min grafting time using 5 kDa PEG-NH_2, 60 °C, 15 mM tris buffer (pH = 8.8). All values were obtained via gravimetric analysis. A 60 min PDOPA deposition (2 mg/mL dopamine, 15 mM tris, pH = 8.8, ambient conditions) was used for all membranes prior to PEG grafting. The results are reported as the mass of PEG added to the membrane per unit nominal surface area of the membranes. The internal surface area of this membrane is not known, so it could not be used to normalize the grafting mass results.

and smooth. The graft densities reported in this work are based on nominal surface areas and do not reflect the internal surface area of the membranes. For example, Ulbricht et al. reported a surface area, measured via BET nitrogen adsorption, of 23.1 m^2/g for a polypropylene MF membrane (0.4 μm pore diameter), which corresponds to an effective surface area of 760 m^2 per m^2 of membrane (165 μm thickness, membrane density of 0.2 g/cm^3) [25]. Similar surface area values, ranging from approximately 15–23 m^2/g, have been reported for other UF and MF membranes [26,27]. Therefore, assuming that PDOPA deposits on a significant portion of the PS-20 UF pore structure and that the PS-20 UF membranes have an effective surface area similar to other UF membranes, a 5 kDa PEG-NH_2 apparent grafting density of 30 $\mu g/cm^2$ would correspond to an actual grafting density of 0.04 $\mu g/cm^2$, which is slightly higher than the grafting density at the onset of PEG chain overlap. However, even larger polymer grafting densities on membranes have been observed in other studies. As an example, Ulbricht et al. observed PEG methacrylate grafting densities of up to 2000 $\mu g/cm^2$ on polyacrylonitrile (PAN) UF membranes using a UV-induced grafting method, and the presence of these PEG grafts on the PAN surface correlated with significantly reduced protein adhesion [28].

4.2.2. *Influence of PEG-NH_2 molecular weight and PDOPA deposition time on PEG grafting*

To more clearly isolate the influence of PEG grafting on pure water flux, it is useful to consider the hydraulic resistance of the PEG grafting rather than the ratio J_{PEG}/J_{PDOPA}, because, as shown in Fig. 3, J_{PDOPA} increases with increasing PDOPA deposition time. Fig. 6 presents the influence of PDOPA deposition time on R_{PEG} (cf., equation (8)) for PDOPA-modified PVDF MF, PS-20 UF, and XLE RO membranes at three different PEG-NH_2 molecular weights. Grafting densities, measured via gravimetric analysis, are presented in Fig. 7. R_{PEG} values for PDOPA-g-PEG modified PVDF MF membranes were lower than the hydraulic resistances of unmodified and PDOPA-modified membranes (cf., Table 4). These low R_{PEG} values, coupled with the fact that there was no discernable trend between PDOPA deposition or PEG-NH_2 molecular weight and R_{PEG}, indicate that PEG grafting had little effect on the flux of PVDF MF membranes. However, as PDOPA deposition time increased, PEG grafting density did increase for PVDF MF membranes, as shown in Fig. 7. Unfortunately, PDOPA deposition density was difficult to verify using a gravimetric analysis because PDOPA deposited in quantities below the detection limit of this gravimetric technique (i.e.,

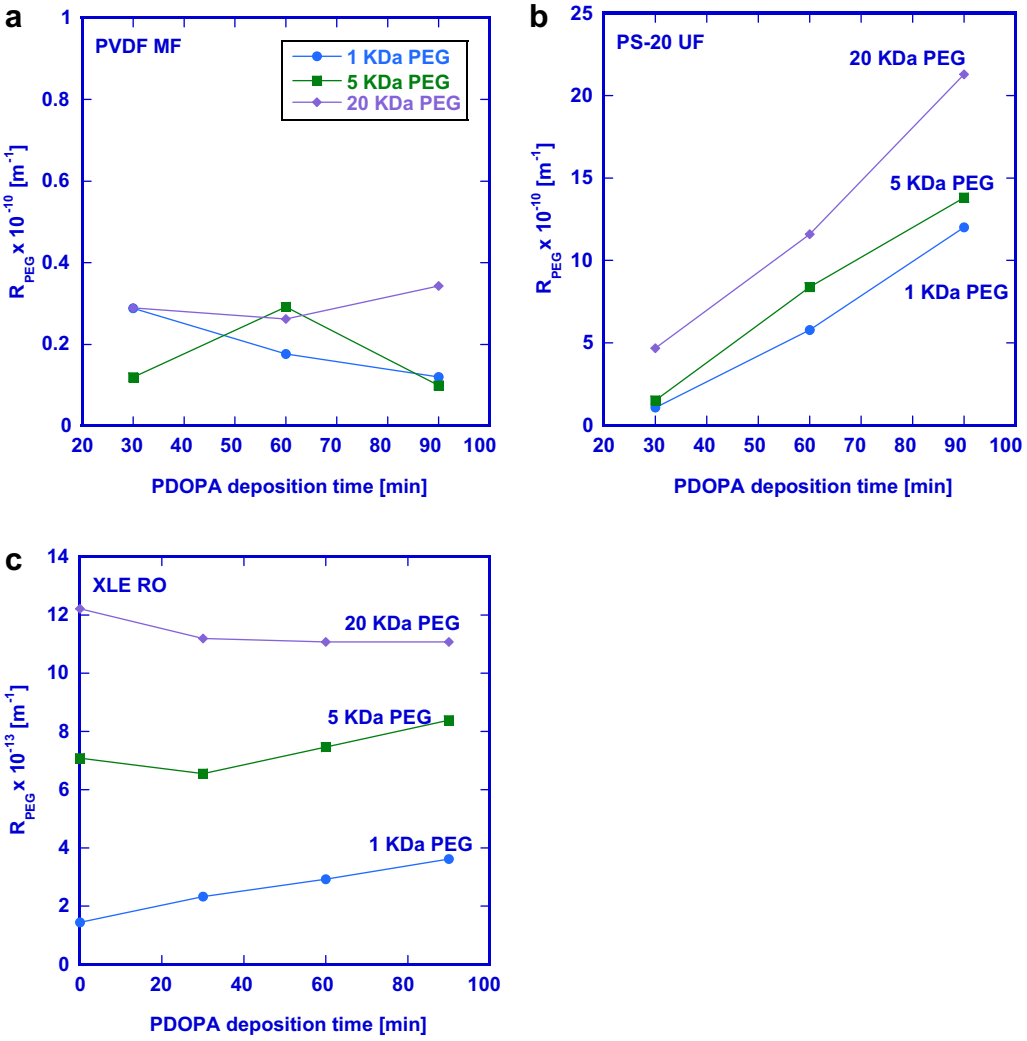

Fig. 6. Hydraulic resistance of PEG grafted to PDOPA-modified: a) PVDF MF, b) PS-20 UF, and c) XLE RO membranes as a function of PDOPA deposition time and PEG-NH_2 molecular weight. PDOPA deposition conditions: 2 mg/mL dopamine in tris buffer (15 mM, pH = 8.8) at ambient conditions. PEG grafting conditions: 60 min (PVDF MF and PS-20 UF) or 30 min (XLE RO) PEG grafting time using 2×10^{-4} mol/L PEG-NH_2, 60 °C, tris buffer (15 mM, pH = 8.8). Standard errors were (in m^{-1}): 1.2×10^9 (PVDF MF), 1.6×10^{10} (PS-20 UF), and 1.0×10^{13} (XLE RO). Standard errors were calculated from at least 2 replicate trials of 4 data points for each membrane.

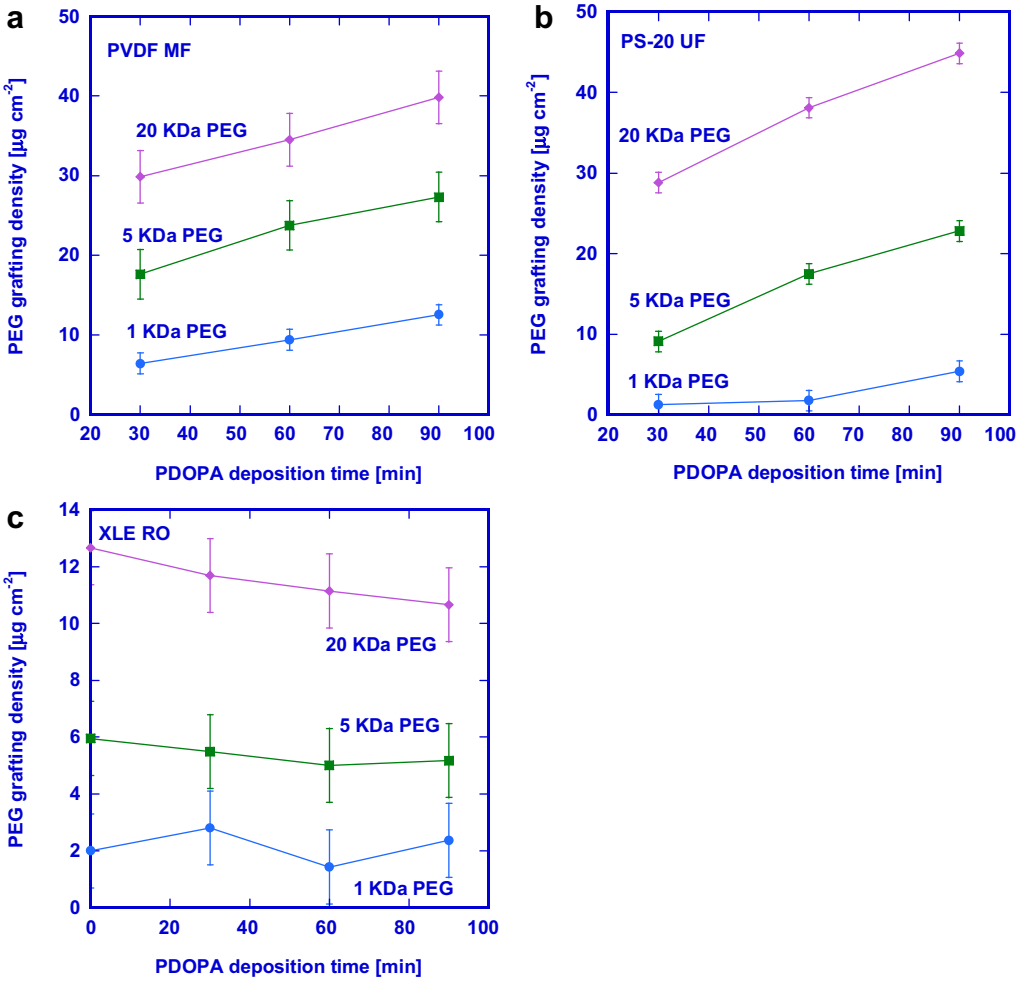

Fig. 7. PEG grafting density as a function of PDOPA deposition and PEG-NH_2 molecular weight on: a) PVDF MF, b) PS-20 UF, and c) XLE RO membranes. All values were obtained via gravimetric analysis. PDOPA deposition conditions: 2 mg/mL dopamine in tris buffer (15 mM, pH = 8.8) at ambient conditions. PEG grafting conditions: 60 min (PVDF MF and PS-20 UF) or 30 min (XLE RO) PEG grafting time using 2×10^{-4} mol/L PEG-NH_2, 60 °C, tris buffer (15 mM, pH = 8.8). Error bars are the standard error of at least two replicate trials.

<1 µg cm^{-2}). Furthermore, as expected, higher PEG-NH_2 molecular weights led to increased grafting densities. Nevertheless, probably because the PVDF MF pore size was large relative to the PDOPA layer thickness and the length of grafted PEG chains, an increase in PEG grafting density had little to no effect on flux.

PDOPA-modified PS-20 UF membranes exhibited similar trends and magnitudes in PEG grafting density as PDOPA-modified PVDF MF membranes: PEG grafting density increased as both PDOPA deposition time and PEG-NH_2 molecular weight increased. However, in contrast to the results from the PVDF MF membrane, the increase in PEG grafting density resulted in an increase in R_{PEG} for the PS-20 UF membrane, and the hydraulic resistance was higher in PDOPA-g-PEG samples than in unmodified or PDOPA-modified samples, as shown in Table 4.

The XLE RO membranes have excess carboxylic acid functionality on their surfaces as a byproduct of the interfacial polymerization method used to synthesize the membrane [29]. The carboxylic acids moieties can react and form covalent linkages with PEG-NH_2 [30]. PVDF MF and PS-20 UF membrane have no such reactive moieties. Therefore, PEG grafting was also characterized on unmodified XLE RO membranes. PEG grafting (without prior PDOPA deposition) to XLE RO membranes was performed by placing unmodified membranes in a 2×10^4 mol/L solution of 1, 5, or 20 kDa PEG-NH_2 (15 mM tris buffer, pH = 8.8, 60 °C) for 30 min. Although PEG grafting densities on PDOPA-modified XLE RO were significantly lower than on PDOPA-modified PVDF MF or PS-20 UF membranes (cf., Fig. 7), the decrease in flux (i.e., increase in resistance) associated with PEG grafting is more significant in the XLE RO membranes (as seen by the high R_{PEG} values, which are, in the case of 20 kDa PEG-NH_2, 3 times higher than the hydraulic resistance of an unmodified XLE RO membrane). No PEG grafting-associated flux loss was observed as PDOPA deposition time increased. Moreover, PEG grafting density remained essentially constant as PDOPA deposition time increased. Perhaps PDOPA deposition shields reactive carboxylic acid sites and makes reactive catechol/quinone sites available to the PEG-NH_2, with the net result being not much change in the number of reactive sites on the RO membrane surface for the PEG-NH_2. Thus, in contrast to the results obtained using the PVDF MF and PS-20 UF membranes, PDOPA deposition did not measurably increase PEG grafting to XLE RO membranes.

4.2.3. BSA adhesion resistance

As a first step towards assessing the ability of PDOPA and PDOPA-g-PEG surface treatment to alter protein adhesion to membranes, fluorescently tagged BSA adhesion experiments were performed on unmodified, PDOPA-modified, and PDOPA-g-PEG modified membranes. The method used in this study is a modified version of a similar method reported in the literature [31]. Organic adhesion to membranes is a necessary step in any fouling process

[32,33]. Protein adhesion, in particular, to membranes is problematic because it primes the surface for and provides a nutrient source for biofilm-forming bacteria, which can lead to catastrophic flux reductions in membranes used for wastewater treatment or thrombosis in membranes used for applications in medical-related fields, such as hemodialysis [32–34]. Of course, the measurements reported here should be complemented by filtration experiments involving protein solutions to determine the fouling resistance, and those studies are under way now in our laboratories.

Fig. 8 presents the influence of PDOPA deposition time and PEG molecular weight on the relative amount of BSA adhered to the membranes. The amount of BSA on the membranes is characterized as the ratio of the fluorescent intensity of BSA adhered to modified membranes, I, to that of BSA adhered to their unmodified analogs, I_o. For the unmodified membranes, protein adhesion was in the following order:

PS-20 UF > PVDF MF > XLE RO.

This trend was also observed in previous studies that considered longer contact times between membranes and protein solutions [2]. PDOPA-only modified membranes are labeled “No PEG” in these plots. BSA adhesion to the PDOPA-modified membranes was significantly lower than that of the unmodified membranes. For example, a PVDF MF membrane, subjected to 30 min of PDOPA deposition, exhibited 83% lower BSA adhesion than its unmodified analog, and the reduction in BSA adhesion was even greater after longer PDOPA deposition times. In the case of a PS-20 UF membrane subjected to 90 min of PDOPA deposition, the BSA adhesion was reduced by more than 99.9% compared to that of its unmodified analog. PDOPA modification also significantly reduced protein adhesion to XLE RO membranes, which already exhibited low protein adhesion [2] due to their high hydrophilicity and negative charge. BSA is also negatively charged at neutral to alkaline pH, and both of these factors (i.e., hydrophilicity and negative surface charge) have been linked to decreased BSA adhesion [9]. Furthermore, protein adhesion was reduced as PDOPA deposition time increased for all membranes.

Protein adhesion reduction by PDOPA deposition is interesting given the chemical nature of PDOPA, which was designed to mimic an adhesive protein [1]. The reduction in protein adhesion could occur as a result of the formation of a small number of PDOPA brushes, in a manner analogous to previously reported physisorbed polymers [35], that might be found throughout the PDOPA layer,

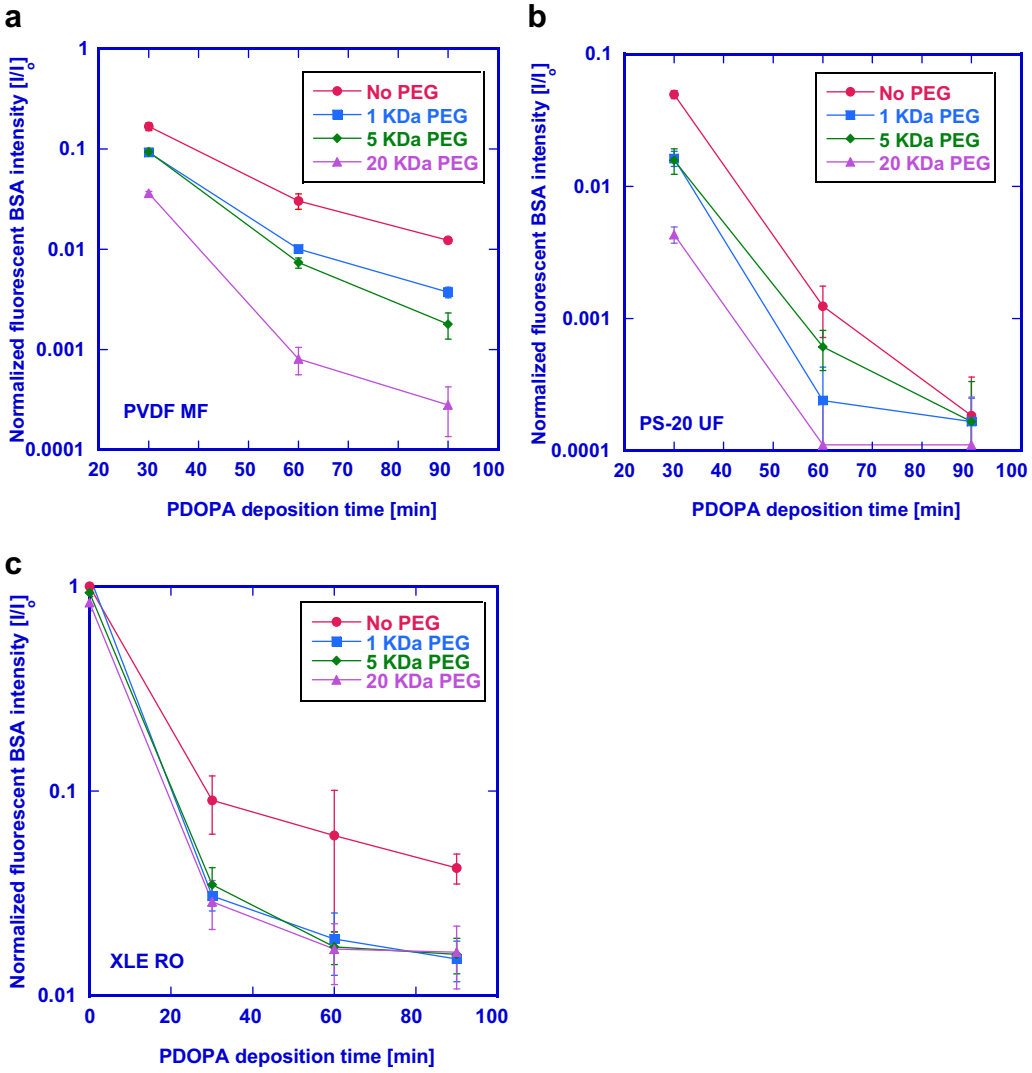

Fig. 8. Influence of PDOPA deposition time on normalized fluorescent intensity of BSA adhered to: a) PVDF MF, b) PS-20 UF, and c) XLE RO membranes. Rhodamine-tagged BSA was used, and the intensity of the BSA adhered to the membrane was measured using $\lambda_{ex}/\lambda_{em}$ = 525 nm/575 nm and a plate reader. All intensities were normalized to the adhered BSA intensity measured on an unmodified membrane.

coupled with the fact that PDOPA is a highly hydrophilic substance. Hydrogen bonding between the hydrophilic catechol group in PDOPA and water molecules could lead to steric hinderance of proteins approaching the surface, which would render adhesion to the PDOPA surface difficult [36–38]. This mechanism of protein adhesion resistance is reminiscent of that reported for PEG brushes [37,38]. However, PDOPA could probably react to form covalent bonds with protein amino acid residues, such as lysine, arginine, and cysteine, under alkaline conditions (our BSA adhesion tests were performed at neutral pH) [39]. Therefore, PEG grafting may be needed to minimize protein adhesion over a broad pH range.

As indicated in Fig. 8, PEG grafting to the PDOPA layer further decreased BSA adhesion relative to PDOPA-modified membranes. Overall, BSA adhesion decreased with increasing PDOPA deposition time in both PDOPA and PDOPA-g-PEG modified membranes. In PVDF MF membranes, a general trend of decreasing BSA adhesion with increasing PEG molecular weight was observed, with 20 kDa PDOPA-g-PEG-modified membranes exhibiting the lowest BSA adhesion for each PDOPA deposition time. All PDOPA-g-PEG modified PVDF MF membranes with a PDOPA modification time of 60 or 90 min exhibited more than 99% reduction in protein adhesion compared to that of unmodified PVDF MF membranes. For PS-20 membranes, 20 kDa PEG also provided the best resistance to BSA adhesion. PDOPA-modified PS-20 UF membranes subjected to 90 min of PDOPA modification exhibited essentially no measurable protein adhesion, so grafting PEG to this membrane resulted in no measurable reduction in BSA adhesion, at least according to the adhesion assay used in this study. PEGs of various molecular weights resulted in nearly identical reductions in BSA adhesion in PDOPA-g-PEG modified XLE RO membranes.

The synergistic protein adhesion resistance of combining PDOPA deposition and PEG grafting may be further elucidated by comparing protein adhesion to PEG-modified XLE RO membranes (i.e., membranes with no PDOPA deposition prior to PEG modification) and to PDOPA-g-PEG modified XLE RO membranes. Among the family of XLE RO membranes modified with only PEG (i.e., with no PDOPA), the membranes modified with 20 kDa PEG-NH_2 exhibited a 17% reduction in BSA adhesion compared to that of an unmodified analog. No reduction in BSA adhesion was observed upon modification with 1 kDa PEG-NH_2, and a 10% reduction was observed when the membrane was modified with 5 kDa PEG-NH_2. In contrast, the PDOPA-g-PEG treatment reduced BSA adhesion between 96 and 99% relative to that of unmodified XLE RO membranes.

At the high PEG grafting densities observed in our study, no definitive trend is observed between PEG grafting density and BSA adhesion reduction due solely to PEG adhesion (i.e., the difference in BSA adhesion between PDOPA-modified and PDOPA-g-PEG modified membranes). It is difficult to compare BSA adhesion reduction as a function of PEG grafting density from the data in Fig. 8 because the technique used to control grafting density (i.e., PDOPA deposition time) significantly influences BSA adhesion. Consequently, a series of experiments were performed where PEG grafting time and PEG-NH_2 concentration in the grafting solution were varied to control the PEG grafting density (as seen in Fig. 5 for PS-20 UF membranes). Fig. 9 presents BSA adhesion to PDOPA-modified and PDOPA-g-PEG modified membranes as a function of PEG grafting time and PEG-NH_2 concentration in the grafting solution. All membranes were initially subjected to a 60 min PDOPA modification at the conditions set forth in Materials and Experimental Methods section. The points at a PEG-NH_2 grafting time or concentration of zero correspond to BSA adhesion on membranes only subjected to PDOPA modification. Other than the initial decrease in BSA adhesion upon exposing the membranes to PEG, only a small reduction in BSA adhesion was observed for PVDF MF membranes as PEG grafting time and concentration increased. For PS-20 UF and XLE RO membranes, BSA adhesion showed no definitive trend with PEG grafting time and concentration. Therefore, PEG surface coverage, regardless of grafting time or concentration, is sufficiently high to give high levels of BSA adhesion resistance, at least within the limits of detection of BSA adhesion used in this work. Since PEG deleteriously influences flux in the UF and RO membranes, this result suggests that membranes prepared with as low a PEG concentration as possible may be of most interest for retaining high flux and significant fouling resistance.

4.2.4. Correlation between BSA adhesion resistance and total flux loss due to PDOPA or PDOPA-g-PEG

One objective of this study was to evaluate the tradeoff between improved BSA adhesion resistance characteristics and the reduction in flux accompanying the membrane modifications

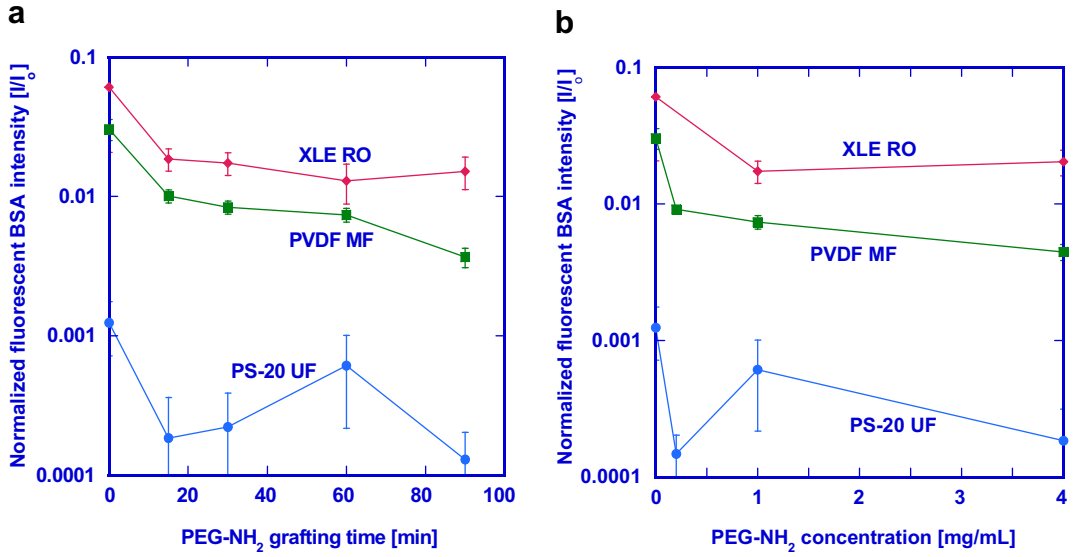

Fig. 9. Influence of a) PEG grafting time and b) PEG-NH_2 concentration in the grafting solution on normalized fluorescent intensity of BSA adhered to PVDF MF, PS-20 UF, and XLE RO membranes. Prior to PEG grafting, these membranes were first PDOPA-modified using a 60 min PDOPA deposition time at ambient conditions and the following dopamine solution: 2 mg/mL, 15 mM tris buffer, pH = 8.8.

considered. Ideally, one would seek membrane modifications that yielded the maximum reduction in BSA adhesion and the minimum reduction in flux. In Fig. 10, a measure of the reduction in BSA adhesion, characterized as $1 - I/I_o$, is plotted against the ratio of the modified membrane's pure water flux, J_T, relative to the flux of its unmodified analog, J_o. An ideal modification would result in membranes having a BSA adhesion reduction of 1 (corresponding to an I value of 0, indicating no BSA adhesion on the modified membrane) and the same flux as an unmodified membrane ($J_T/J_o = 1$). As a result, values closest to the upper right corner of Fig. 10 are desirable. The PVDF MF membranes show the best combinations of flux retention and enhancement in resistance to protein adhesion, in part because their large pores allow these membrane modifications to occur with little loss in flux. The UF membranes show very good resistance to protein adhesion, but flux can be significantly reduced by extensive modification since these membranes have smaller pores, which are more easily constricted or bridged by the modifications considered, than those of the MF membranes. The XLE RO membranes show a distinct tradeoff, with more significant modification conditions (i.e., high-density PEG grafting) yielding substantial improvements in protein adhesion resistance but large reductions in flux. In general, the XLE RO membranes show the least improvement in protein adhesion resistance for a given reduction in flux, presumably because of unmodified XLE RO's already low comparative protein adhesion.

Table 5 provides some examples of the detailed modification conditions characterizing this tradeoff. In the PS-20 UF membranes, which have smaller pore size that the PVDF MF membranes, many of the most effective modification conditions, from a BSA adhesion reduction standpoint (i.e., $1 - I/I_o$ values closest to 1), showed significant reductions in flux, and the most effective modification conditions (from a point of view of balancing BSA adhesion resistance and flux loss) had a combination of PDOPA deposition and PEG grafting. The XLE RO membranes showed the clearest evidence of a distinct tradeoff between BSA adhesion resistance and flux, and modifications involving PEG grafting generally gave the most significant reductions in flux. In summary, PDOPA deposition, combined with PEG grafting, provides an effective tool for modifying membrane surfaces, and the balance of flux reduction and protein adhesion resistance must be determined experimentally for each membrane of interest.

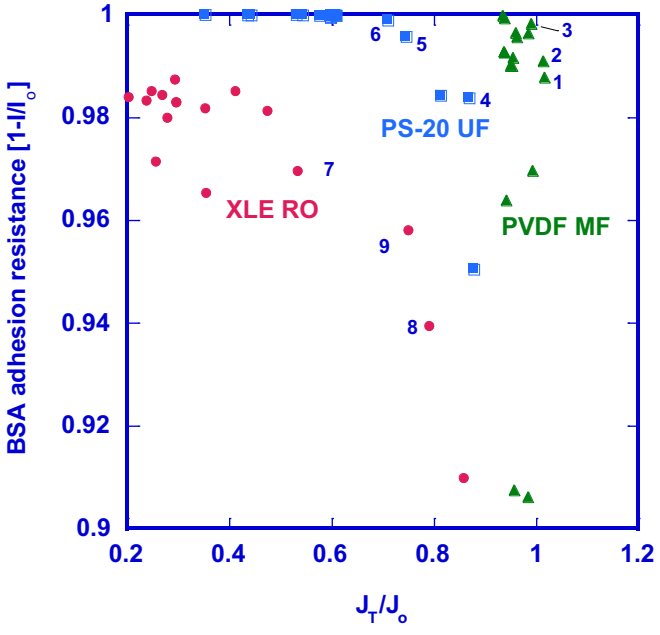

Fig. 10. BSA adhesion reduction as a function of the ratio of modified membrane flux, J_T, to the unmodified membrane flux, J_o. (●): XLE RO, (■): PS-20 UF, (▲): PVDF MF.

Table 5
Modification parameters for membranes numbered in Fig. 10.

Label from Fig. 1.10	Membrane	PDOPA deposition time [min]	PEG-NH_2 grafting time [min]	PEG-NH_2 concentration [mg/ml]	PEG-NH_2 molecular weight [kDa]
1	PVDF MF	90	0	NA	NA
2	PVDF MF	30	60	4	20
3	PVDF MF	60	0	NA	NA
4	PS-20 UF	90	0	NA	NA
5	PS-20 UF	60	60	0.2	1
6	PS-20 UF	90	60	1	5
7	XLE RO	30	30	0.2	1
8	XLE RO	60	0	NA	NA
9	XLE RO	90	0	NA	NA

5. Conclusions

PVDF MF, PSF A1 and PS-20 UF and XLE RO membranes were modified using PDOPA. PEG-NH_2 could be grafted to PDOPA-modified membranes. PDOPA and PDOPA-g-PEG modifications influenced pure water flux differently in each membrane. For example, PDOPA and subsequent PEG grafting had little influence on PVDF MF membrane flux because the pore size of these membranes was likely to be much larger than the thicknesses of the PDOPA deposition and the PEG graft layer. However, a decrease in PS-20 UF water flux was observed with increasing PDOPA deposition and PEG grafting density, probably because the pore size of these membranes was similar to the PDOPA deposition and PEG graft layer thicknesses. XLE RO membranes exhibited a small decrease in flux with increasing PDOPA deposition (most likely due to a low amount of PDOPA deposition compared to the other membranes considered), but PEG grafting significantly reduced XLE RO flux. PDOPA deposition substantially reduced BSA adhesion in all cases. Additional BSA adhesion reduction was observed when PEG was grafted to the membrane. A general trend of reduced BSA adhesion with increasing PEG graft molecular weight was observed for all membranes, except for the XLE RO, where all molecular weights of grafted PEG exhibited similar BSA adhesion. Finally, by plotting BSA adhesion resistance as a function of total unmodified membrane flux retained after a modification, a tradeoff between protein adhesion resistance and pure water flux was observed for several membranes.

Acknowledgements

The authors gratefully acknowledge support from the National Science Foundation (Graduate Research Fellowships for Mr. McCloskey and Mr. Miller, the Center for Layered Polymer Systems, grant DMR 0423914) and Advanced Hydro, Inc. We also wish to acknowledge Professors Young Moo Lee and Heungsoo Shin of Hanyang University for their support of our studies through a National Science Foundation IREE (International Research and Education in Engineering) fellowship for Mr. McCloskey. The original project for the IREE fellowship was "Collaborative Research: A Polymer Synthesis/Membrane Characterization Program on Fouling Resistant Membranes for Water Purification" (CBET 0553957). Additional support from NSF CBET-0931761 and the Research Partnership to Secure Energy for America (RPSEA) (Department of Energy Contract Number DE-AC26-07NT2677), via subcontract from the Gas Technologies Institute, is gratefully acknowledged. H.B. Park acknowledges support from the SMBA project (grand #31200900000560001).

References

[1] Lee H, Dellatore SM, Miller WM, Messersmith PB. Mussel-inspired surface chemistry for multifunctional coatings. Science 2007;318:426–30.
[2] McCloskey BD, Novel surface modifications and materials for fouling resistant water purification membranes, PhD thesis, University of Texas at Austin, 2009.
[3] Belfort G, Davis RH, Zydney AL. The behavior of suspensions and macromolecular solutions in crossflow microfiltration. Journal of Membrane Science 1994;96:1–58.
[4] Cheryan M. Microfiltration and ultrafiltration handbook. Lancaster, PA: Technomic Publishing; 1998.
[5] Kelly ST, Zydney AL. Mechanisms for BSA fouling during microfiltration. Journal of Membrane Science 1995;107:115–27.
[6] Ho C-C, Zydney AL. Effect of membrane morphology on the initial rate of protein fouling during microfiltration. Journal of Membrane Science 1999;155:261–75.
[7] Bowen WR, Quan G. Properties of microfiltration membranes: flux loss during constant pressure permeation of bovine serum albumin. Biotechnology and Bioengineering 1991;38:688–96.
[8] Mueller J, Davis RH. Protein fouling of surface-modified polymeric microfiltration membranes. Journal of Membrane Science 1996;116:47–60.
[9] Ostuni E, Chapman RG, Holmlin RE, Takayama S, Whitesides GM. A survey of structure–property relationships of surfaces that resist the adsorption of protein. Langmuir 2001;17:5605–20.
[10] Wiesner MR, Aptel P. Mass transport and permeate flux and fouling in pressure-driven processes. In: Water treatment: membrane processes. New York, NY: McGraw Hill Co.; 1996. 4.1–30.
[11] Wijmans JG, Baker RW. The solution–diffusion model: a review. Journal of Membrane Science 1995;107:1–21.
[12] Ju H, McCloskey BD, Sagle AC, Wu Y-H, Kusuma VA, Freeman BD. Crosslinked poly(ethylene oxide) fouling resistant coating materials for oil/water separation. Journal of Membrane Science 2008;307:260–7.
[13] Van Wagner EM, Sagle AC, Sharma MM, Freeman BD. Effect of crossflow testing conditions, including feed pH and continuous feed filtration, on commercial reverse osmosis membrane performance. Journal of Membrane Science 2009;345:97–109.
[14] Rowe BW, Freeman BD, Paul DR. Physical aging of ultrathin glassy polymer films tracked by gas permeability. Polymer 2009;50:5565–75.
[15] Papanu JS, Hess DW, Bell AT, Soane DS. In situ ellipsometry to monitor swelling and dissolution of thin polymer films. Journal of the Electrochemical Society 1989;136:1195–200.
[16] Huang Y, Paul DR. Experimental methods for tracking physical aging of thin glassy polymer films by gas permeation. Journal of Membrane Science 2004;244:167–78.
[17] Amine Reactive Probes. Molecular Probes, Inc., http://probes.invitrogen.com/media/pis/mp00143.pdf; Feb 2010.
[18] Singh S, Khulbe KC, Matsuura T, Ramamurthy P. Membrane characterization by solute transport and atomic force microscopy. Journal of Membrane Science 1998;142:111–27.
[19] Li B, Liu W, Jiang Z, Dong X, Wang B, Zhong Y. Ultrathin and stable active layer of dense composite membrane enabled by poly(dopamine). Langmuir 2009;25:7368–74.
[20] Le-Clech P, Chen V, Fane TAG. Fouling in membrane bioreactors used in wastewater treatment. Journal of Membrane Science 2006;284:17–53.
[21] Deshmukh SP, Li K. Effect of ethanol composition in water coagulation bath on morphology of PVDF hollow fibre membranes. Journal of Membrane Science 1998;150:75–85.
[22] Taniguchi M, Belfort G. Low protein fouling synthetic membranes by UV-assisted surface grafting modification: varying monomer type. Journal of Membrane Science 2004;231:147–57.
[23] Mickols WE. Composite membrane with polyalkylene oxide modified polyamide surface. United States Patent #6,280,853; 2001.
[24] Malmsten M, Emoto K, Van Alstine JM. Effect of chain density on inhibition of protein adsorption by poly(ethylene glycol) based coatings. Journal of Colloid and Interface Science 1998;202:507–17.
[25] Borcherding H, Hicke H-G, Jorcke D, Ulbricht M. Affinity membranes as a tool for life science applications. Annals of the New York Academy of Sciences 2003;984:470–9.
[26] Ramamoorthy M, Ulbricht M. Molecular imprinting of cellulose acetate–sulfonated polysulfone blend membranes for Rhodamine B by phase inversion technique. Journal of Membrane Science 2003;217:207–14.
[27] Han M-J. Effect of propionic acid in the casting solution on the characteristics of phase inversion polysulfone membranes. Desalination 1999;121:31–9.
[28] Ulbricht M, Matuschewski H, Oechel A, Hicke H-G. Photo-induced graft polymerization surface modifications for the preparation of hydrophilic and low-protein-adsorbing ultrafiltration membranes. Journal of Membrane Science 1996;115:31–47.
[29] Sagle AC, Van Wagner EM, Ju H, McCloskey BD, Freeman BD, Sharma MM. PEG-coated reverse osmosis membranes: desalination properties and fouling resistance. Journal of Membrane Science 2009;340:92–108.
[30] Kang G, Liu M, Lin B, Cao Y, Yuan Q. A novel method of surface modification on thin-film composite reverse osmosis membrane by grafting poly(ethylene glycol). Polymer 2007;48:1165–70.
[31] Taylor M, Urquhart AJ, Anderson DG, Williams PM, Langer R, Alexander MR, et al. A methodology for investigating protein adhesion and adsorption to microarrayed combinatorial polymers. Macromolecular Rapid Communications 2008;29:1298–302.
[32] Hasegawa T, Iwasaki Y, Ishihara K. Preparation and performance of protein-adsorption-resistant asymmetric porous membrane composed of polysulfone/phospholipid polymer blend. Biomaterials 2001;22:243–51.
[33] Higuchi A, Sugiyama K, Yoon BO, Sakurai M, Hara M, Sumita M, et al. Serum protein adsorption and platelet adhesion on pluronic (TM)-adsorbed polysulfone membranes. Biomaterials 2003;24:3235–45.
[34] Percival SL, Walker JT, Hunter PR. Microbiological aspects of biofilms and drinking water. New York, NY, USA: CRC Press; 2000.
[35] Reddy AVR, Mohan DJ, Bhattacharya A, Shah VJ, Ghosh PK. Surface modification of ultrafiltration membranes by preadsorption of a negatively charged polymer: I. Permeation of water soluble polymers and inorganic salt solutions and fouling resistance properties. Journal of Membrane Science 2003;214:211–21.
[36] Ahn DS, Jeon IS, Jang SH, Park SW, Lee S, Cheong W. Hydrogen bonding in aromatic alcohol–water clusters: a brief review. Bulletin of the Korean Chemical Society 2003;24:695–702.
[37] Halperin A. Polymer brushes that resist adsorption of model proteins: design parameters. Langmuir 1999;15:2525–33.
[38] Nath N, Hyun J, Ma H, Chilkoti A. Surface engineering strategies for control of protein and cell interactions. Surface Science 2004;570:98–110.
[39] Lee H, Rho J, Messersmith PB. Facile conjugation of biomolecules onto surfaces via mussel adhesive protein inspired coatings. Advanced Materials 2009;21:431–4.